RESEARCH ARTICLE

WILEY

Unimanual sensorimotor learning—A simultaneous EEG-fMRI aging study

Sabrina Chettouf[1,2,3] | Paul Triebkorn[1,2,4] | Andreas Daffertshofer[3] |
Petra Ritter[1,2,5,6,7]

[1]Berlin Institute of Health at Charité, Universitätsmedizin Berlin, Charitéplatz 1, Berlin, Germany

[2]Department of Neurology with Experimental Neurology, Charité, Universitätsmedizin Berlin, Corporate member of Freie Universität Berlin and Humboldt Universität zu Berlin, Charitéplatz 1, Berlin, Germany

[3]Amsterdam Movement Sciences & Institute for Brain and Behavior Amsterdam, Faculty of Behavioural and Movement Sciences, Vrije Universiteit, Amsterdam

[4]Institut de Neurosciences des Systèmes, Aix Marseille Université, Marseille, France

[5]Bernstein Center for Computational Neuroscience Berlin, Berlin, Germany

[6]Einstein Center for Neuroscience Berlin, Berlin, Germany

[7]Einstein Center Digital Future, Berlin, Germany

Correspondence
Sabrina Chettouf and Petra Ritter, Charité – Universitätsmedizin Berlin, Corporate Member of Freie Universität Berlin, Humboldt-Universität zu Berlin, and Berlin Institute of Health, Department of Neurology, Brain Simulation Section, Robert-Koch-Platz 4, 10115 Berlin, Germany.
Email: s.chettouf@vu.nl and petra.ritter@charite.de

Abstract

Sensorimotor coordination requires orchestrated network activity in the brain, mediated by inter- and intra-hemispheric interactions that may be affected by aging-related changes. We adopted a theoretical model, according to which intra-hemispheric inhibition from premotor to primary motor cortex is mandatory to compensate for inter-hemispheric excitation through the corpus callosum. To test this as a function of age we acquired electroencephalography (EEG) simultaneously with functional magnetic resonance imaging (fMRI) in two groups of healthy adults (younger $N = 13$: 20–25 year and older $N = 14$: 59–70 year) while learning a unimanual motor task. On average, quality of performance of older participants stayed significantly below that of the younger ones. Accompanying decreases in motor-event-related EEG β-activity were lateralized toward contralateral motor regions, albeit more so in younger participants. In this younger group, the mean β-power during motor task execution was significantly higher in bilateral premotor areas compared to the older adults. In both groups, fMRI blood oxygen level dependent (BOLD) signals were positively correlated with source-reconstructed β-amplitudes: positive in primary motor and negative in premotor cortex. This suggests that β-amplitude modulation is associated with primary motor cortex "activation" (positive BOLD response) and premotor "deactivation" (negative BOLD response). Although the latter results did not discriminate between age groups, they underscore that enhanced modulation in primary motor cortex may be explained by a β-associated excitatory crosstalk between hemispheres.

KEYWORDS
aging, coordination, intra-hemispheric inhibition, motor learning, motor network, perceptual motor behavior

1 | INTRODUCTION

Motor coordination requires a fine-tuned interplay of activities across the sensorimotor network. It involves entraining motor commands to integrate sensory information to produce functionally meaningful output. The interplay may be altered by aging-related neurodegeneration (Holtrop, Loucks, Sosnoff, & Sutton, 2014; Sullivan & Pfefferbaum, 2006). Even in seemingly simple tasks like repetitive finger tapping, motor performance is known to decline with increasing age (Shimoyama, Ninchoji, & Uemura, 1990). And, the decline appears more pronounced when motor timing is more demanding or when movements are visually guided (Houx & Jolles, 1993; Kauranen & Vanharanta, 1996; Smith et al., 1999; Ward & Frackowiak, 2003). It might be that in older adults proper motor control comes at the price of widespread involvement of brain regions. Seidler et al. (2010) highlighted an increased engagement of prefrontal cortex and basal ganglia, which both are part of the motor network and are known to be affected by aging-related alterations. Over the years, several studies addressed the effect of aging on the sensorimotor network activity, primarily in (bilateral) primary and premotor areas (Fujiyama et al., 2016; Maes, Gooijers, de Xivry, Swinnen, & Soisgontier, 2017; Seidler et al., 2010; Swinnen & Wenderoth, 2004; Tscherpel et al., 2020). The blood-oxygen-level-dependent (BOLD) contrast from functional magnetic resonance imaging (fMRI) indicated aging to be accompanied by less deactivation of ipsilateral primary motor areas. This suggests a reduced inter-hemispheric inhibition during unimanual movements (Coxon et al., 2010; Goble et al., 2010; Hinder, Fujiyama, & Summers, 2012; Levin, Fujiyama, Boisgontier, Swinnen, & Summers, 2014; Van Impe, Coxon, Goble, Wenderoth, & Swinnen, 2009), which may impair motor control (suppression) of homologous end-effectors (Hutchinson et al., 2002; Newton, Sunderland, & Gowland, 2005; Ward & Frackowiak, 2003).

Inter-limb coordination is a particular form of motor coordination, where different parts of the motor network have to orchestrate their activities. Coordinated movements of the upper extremities are accompanied by bilateral (left/right) cortical activities, even if the motor output is unimanual (Chettouf, Rueda-Delgado, de Vries, Ritter, & Daffertshofer, 2020). The prime interface for left/right interactions is the corpus callosum (CC), which is known for its aging-related changes (Frederiksen & Waldemar, 2012; Langan et al., 2010; Sullivan et al., 2001; Sullivan & Pfefferbaum, 2006). Deterioration of the CC may affect unimanual motor control, as there is accumulating evidence that proper unimanual performance entails the inhibition of ipsilateral motor areas (Daffertshofer, Peper, & Beek, 2005; Ghacibeh et al., 2007; Gross et al., 2005; van Wijk, Beek, & Daffertshofer, 2012; Vercauteren, Pleysier, Van Belle, Swinnen, & Wenderoth, 2008). Trans-callosal pathways are both inhibitory and excitatory (Daffertshofer et al., 2005; Swinnen, 2002). In particular the excitatory ones may cause inter-hemispheric crosstalk that might be visible in the form of (unwanted) mirror movements (Carson, 2005). Suppressing this crosstalk might be realized through intra-hemispheric inhibition in the hemisphere that is supposed to stay inactive. Yet, that inhibition needs to be precisely timed. This process seems to involve supplementary motor and/or premotor areas (SMA and PM1,

respectively) as suggested by studies using transcranial magnetic stimulation (Stinear & Byblow, 2002). In a recent review we outlined a candidate scheme (Figure 1) for the corresponding circuitry (Chettouf et al., 2020). In brief, during unimanual movements the contralateral M1 projects through the CC and excites ipsilateral M1. The same contralateral M1 also projects to ipsilateral PM1, see also Carson (2020). The latter has inhibitory cortico-cortical projections to M1 in the same hemisphere and, if properly timed, suppresses its activity stemming from contralateral M1. Disruption of PM1 activity by, for example, neurodegeneration either in that area or in the CC, may impede this *effective inter-hemispheric inhibition,* hampering unimanual performance and/or causing activation of homologous muscles (Daffertshofer et al. (2005). In the bimanual case, improper PM1 → M1 inhibition may lead to instabilities of the planned motor action (Houweling, Beek, & Daffertshofer, 2010).

With the current study we sought to investigate the proposed imbalance of the effective inter-hemispheric inhibition in the aging brain. This imbalance is expected to be particularly visible during learning a motor task with distinct timing requirements that we here used to contrast groups of younger and older healthy adults.

The fMRI-BOLD response is the result of a mixture of processes. It hence should be viewed as an indirect measure of neuronal function. Interpreting BOLD response can be a challenge. So-called fMRI "deactivations" and "activations", that is, task or regressor correlations with fMRI-BOLD can reflect both neuronal inhibition and excitation, irrespective of whether the correlations are positive or negative (Ritter & Villringer, 2002). In encephalographic assessments, by contrast, phenomena like motor-related (de-)synchronization in, for example, M1 can be clearly assigned to distinct parts of the motor control loop. As said, fMRI-BOLD is an indirect measure as it relies on the assessment of large-scale metabolic and hemodynamic changes. The changes are typically slow (∼seconds). They do not capture neuronal (spiking) activity but are rather a consequence of it (Logothetis, 2008).
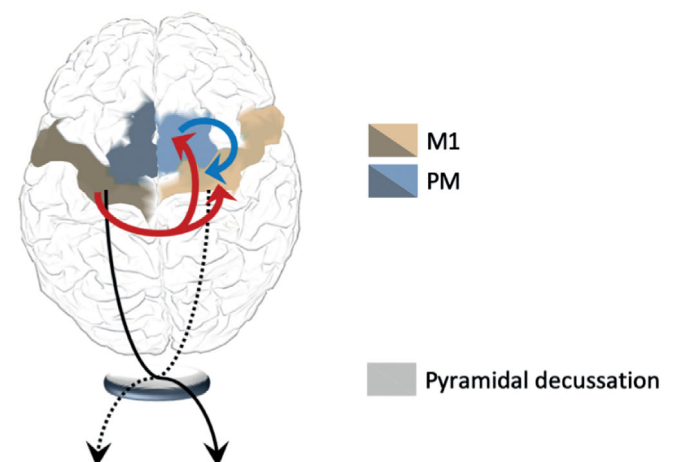

FIGURE 1 From Chettouf et al. (2020). Theoretical model that may account for bilateral cortical activation during unimanual performance. Left M1 activation causes a crosstalk through the corpus callosum in both, right M1 and right PM/SMA, with the latter inhibiting the first to prevent motor outflow to the left (homologous) end-effector

Encephalography allows for identifying incidences of activity to millisecond accuracy and can thus provide insight into the dynamics of, in our case, motor control at high-temporal resolution. In particular, (de-)synchronization in and between neural populations is thought to mediate the functional coupling of the motor network. First and foremost the β-rhythm (around 15–30 Hz) is prominently present in sensorimotor regions (Pfurtscheller, 1981) and the so-called β-rebound (elevated β-power exceeding that of β-activity at rest) is a marker of movement termination. Here we consider motor learning rather than steady motor performance. During motor learning the mean β-activity is known to decrease and, at the same time, motor-related β-modulation increases and synchronization/de-synchronization volleys become more pronounced (Boonstra, Daffertshofer, Breakspear, & Beek, 2007; Houweling, van Dijk, Beek, & Daffertshofer, 2010). As such it is and excellent paradigm for studying the oscillation-based spatiotemporal reorganization across the motor network, as has been highlighted by Rueda-Delgado et al. (2014).

Yet, especially electro-encephalographic (EEG) recordings suffer from poor spatial resolution. After all, neural source activity has to be inferred from surface recordings. MRI imaging provides a formidable spatial resolution in the order of cubic millimeters. We hence combined fMRI and EEG in simultaneous recordings during a sensorimotor task (Ritter, Moosmann, & Villringer, 2009; Ritter & Villringer, 2006; Stevenson, Brookes, & Morris, 2011). The signals of both modalities were first analyzed separately following modality-specific standard approaches. The fMRI provided estimates of region-of-interests (ROIs) relevant for motor performance based on significant changes in BOLD signals. The EEG yielded motor-related activity patterns that revealed parts of the motor network that changed significantly while learning and differed between age groups. Subsequently, the EEG signals served as regressors to identify their correlates in fMRI-BOLD in the hope to find detailed spatial areas responsible for differences in motor learning at different age.

We studied two groups, one with younger and one with older participants. Motor learning was facilitated by simple perceptual cues that we provided by means of visual feedback. We expected both groups to learn a unimanual motor task but learning rate and overall performance to decrease with age. In line with our theoretical model, we hypothesized a less strongly inhibited ipsilateral M1 with increasing age due to a reduced effective inter-hemispheric inhibition. In the older participants we expected a less lateralized motor-related EEG β-band modulation resembling less interhemispheric inhibition during unimanual motor execution (Carson, 2020) irrespective of learning state. For the (EEG and) fMRI analysis we expected more task positive correlated activity in ipsilateral M1 indicating more activation in the older age group, again due to the lack of inhibition.

2 | MATERIALS AND METHODS

2.1 | Participants

Twenty younger adults (mean age = 22.0 years; range, 20–25 years; 13 females) and twenty older adults (mean age = 63.6; range = 59–70 years; 14 females) participated in the study. None of the participants had a history of neurological, psychiatric, or chronic somatic diseases. None of them had musical background, which is known for altered motor timing and accompanying neural activity (Hughes & Franz, 2007). All participants were right-handed according to the Edinburgh Handedness Inventory test (Oldfield, 1971) and the did not show any cognitive impairment assessed with the Montreal Cognitive Assessment (Nasreddine et al., 2005). They gave written informed consent prior to assessment. The experiments were performed in compliance with the relevant laws and institutional guidelines and were approved by the medical ethical committee of the Charité Medical Center in Berlin (EA1/060/14).

2.2 | Experimental design

We adopted a motor learning protocol that was successfully implemented in previous MEG studies (Houweling, Daffertshofer, van Dijk, & Beek, 2008; Houweling, van Dijk, et al., 2010). Participants had to learn a polyrhythmic motor task while online visual feedback was provided. The visual feedback formed a "simple" perceptual goal, cf. Figure 2. Providing such a perceptual goal is known to vastly accelerate motor learning (Mechsner, Kerzel, Knoblich, & Prinz, 2001; Repp, 2005; Swinnen, 2002), which renders it particularly useful for learning complex behavior during limited scanning times. We modified this protocol to unimanual motor learning in the MR scanner.

Participants were asked to squeeze in an air-filled rubber bulb with their right hand in a 4:3 frequency ratio to an external cue. The cue was provided visually by a disc that rotated at 1.8 Hz on a computer display (left). Squeezing the bulb let a second disc (right) rotate (Figure 2). Their squeezing rhythm, however, was mapped in such a way that the two discs rotated at the same frequency, if the cue/performance ratio was 4:3. Put differently, participants had to perform rhythmic squeezing at a frequency of 1.35 Hz for 2 min to achieve a 1:1 left/right disc rotation which can be consider the aforementioned perceptual goal.

In the MR-scanner, 700 volumes were recorded while participants performed a total of 10 trials of 2 min each, separated by 15 s breaks. To reduce motion artifacts, the participant's head was restrained using foam pads. EOG electrodes were recorded to measure eye blinks. Participants were instructed to keep their eyes open during the entire experiment and minimize eye and head movements. After data collection, data containing excessive head movements in the MRI scanner (more than 4 mm) were excluded from analysis. Remaining movement artifacts were removed during offline preprocessing. Blocks of 5 min resting state recordings that served as baseline were collected before and after the motor task. There, participants were instructed to close their eyes but stay awake and to not move their head. On the consecutive day, participants performed the motor task outside the scanner, which served as retention test for verifying motor learning rather than mere non-lasting training effects (Kantak & Winstein, 2012).
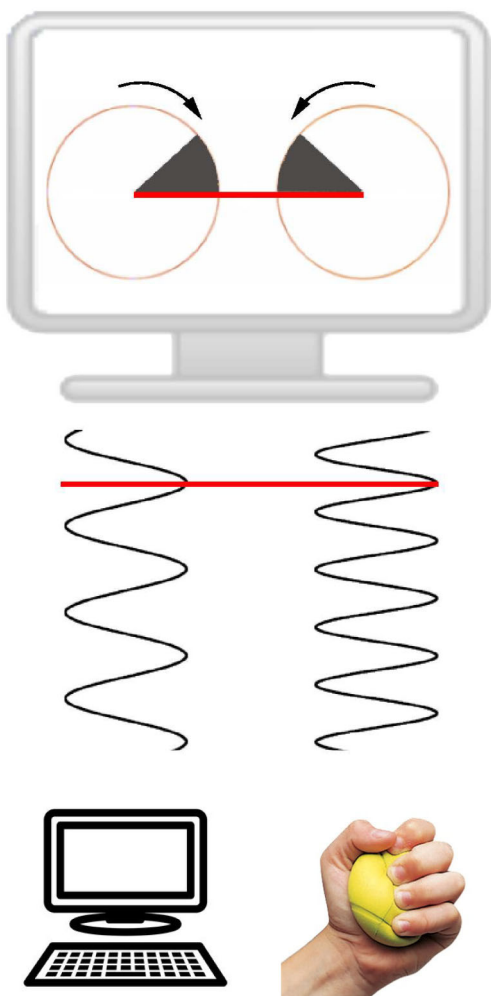
FIGURE 2 Experimental setup. External cue and force performed by the subject were displayed as two rotating discs on a computer screen that was projected via a mirror mounted on top of the head coil to the participant lying in the scanner. Squeezes of the rubber bulb with the right hand were analyzed in real time for the phase dynamics, which was multiplied by a factor 4/3. By this, proper performance of a 4:3 polyrhythm let the disks counter rotate with a 1:1 frequency ratio, which was typically realized in sync; scheme has been modified from Houweling et al. (2008) and Houweling, van Dijk, et al. (2010)

2.3 | Data acquisition

Data have been acquired at the Berlin Center for Advanced Imaging at the Charité Universitätsmedizin Berlin.

2.3.1 | Motor behavior

We used a custom-made pressure transducer to convert the pressure inside an air-filled rubber bulb to an electrical signal that was sampled at a rate of 100 Hz (SCXI module, National Instruments, Austin, USA).

2.3.2 | EEG

EEG recordings were conducted with a 64-channel MR-compatible EEG system (Brain Products, Gilching, Germany; 0.1–250 Hz hardware band-pass filter, ±16.38 mV recording range at a 0.5 µV resolution and 5 kHz sampling rate) and an EEG cap with ring-type sintered silver chloride electrodes with iron-free copper leads (EasyCap, Herrsching, Germany). Sixty-one scalp electrodes were arranged based on the international 10–20 system with FCz as reference and ground electrode at AFz. In addition, two electrocardiogram (ECG) electrodes and one vertical electro-oculogram (EOG) were recorded. An abrasive electrolyte gel (Abralyt 2000, Easycap, Herrsching, Germany) served to keep the impedances of all electrodes below 5 kΩ. The EEG-sampling was synchronized to the gradient-switching clock of the MR scanner, to ensure time-invariant sampling of the image acquisition artifact (SyncBox, Brain Products, Gilching, Germany) (Anami et al., 2003; Freyer et al., 2009).

2.3.3 | (f)MRI

We used a 3 T Siemens Tim Trio MR scanner with a 12-channel Siemens head coil. Every scan session started with a localizer sequence (TR 20 ms, TE 5 ms, 3 slices [8 mm], voxel size $1.9 \times 1.5 \times 8.0$ mm, FA 40°, FoV 280 mm, 192 matrix) followed by an anatomical T1-weighted scan (TR/TE 1900/2.52 ms, FA 9°, 192 sagittal slices [1.0 mm], voxel size $1 \times 1 \times 1$ mm^3, FoV 256 mm, 256 matrix), an anatomical T2-weighted scan (TR 2640 ms, TE1 11 ms, TE2 89 ms, 48 slices [3.0 mm], voxel size $0.9 \times 0.9 \times 3$ mm, FoV 220 mm, 256 matrix). Afterwards, the EEG was prepared; fMRI (BOLD-sensitive, T2*-weighted, TR/TE 1940/30 ms, FA 78°, 32 transversal slices [3 mm], voxel size $3 \times 3 \times 3$ mm, FoV 192 mm, 64 matrix) was recorded simultaneously to the EEG.

2.4 | Data analysis

Data were analyzed using Matlab (version 2017b, The Mathworks, Natwick, MA). For the (f)MRI processing we employed FreeSurfer (version 6.0.0, Laboratory for Computational Neuroimaging, Boston, United States, see Fischl (2012)) the FMRIB (Functional MRI of the Brain) Software Library [version 5.0, Analysis Group, Oxford, UK, see Jenkinson, Beckmann, Behrens, Woolrich, and Smith (2012)], connectome workbench (version 1.2.3, WU-Minn HCP Consortium, USA, see Marcus et al. (2011)) and the preprocessing scripts of the human connectome project (version 3.24.0, WU-Minn HCP Consortium, USA, Glasser et al. (2016, 2013)).

2.4.1 | Motor behavior

We quantified performance via the strength of frequency locking between the visual cue and the force produced. As corresponding

measure we used the normalized spectral overlap (Daffertshofer, Peper, & Beek, 2000), that is, the similarity ψ_x^y between the power spectrum of the cueing signal, P_x, and that of the produced force, P_y, after rescaling the frequency axis by the factor $\rho = p : q$. This measure reads

$$\psi_x^y(\rho) = \frac{2 \int P_x(\omega) P_y(\rho\omega) d\omega}{\int \left[P_x^2(\omega) + P_y^2(\rho\omega) \right] d\omega}$$

It is bounded to the interval [0,1] with 1 indicating maximum similarity. We Fisher-transformed this value prior to statistical evaluation to stabilized normality.

Statistical analysis of the behavioral data was performed with SPSS (IBM Corp. Released 2015. IBM SPSS Statistics for Macintosh, Version 23.0 Armonk, NY, United States: IBM Corp.). Frequency locking values per trial for both groups were subjected to an ANOVA with repeated measures. Within-subject factors were the 10 task trials and the retention test. Age group was included as between-subject factor. The significance threshold was set to $\alpha = 0.05$. Sphericity was tested using Mauchly's test and, when violated, we applied a Greenhouse–Geisser's correction. Post hoc *t*-tests were performed whenever a main effect of Age or Trial was detected to evaluate effects of motor learning. In the first case we applied an independent samples *t*-test between age groups and in the latter case a dependent *t*-test on trials.

2.4.2 | Preprocessing EEG and fMRI

EEG data were segmented with BrainVision Analyzer software (Brain Products) into three parts: the experimental learning task, pre- and post-motor task resting state. We removed MR-scanner artifacts as detailed in Supplementary Material S1, down-sampled to 512 Hz after anti-aliasing filtering, and finally band-pass filtered between 0.1 and 100 Hz. Subsequent EEG preprocessing consisted of removing and interpolating bad channels, removing the ballisto-cardiogram (pulsatile blood movement causing body and electrode movement inside the scanner) and excessive eye blinks as well as movement artifacts using independent component analysis (ICA) (Hyvarinen, 1999). Since ballistocardiograph artifacts can generally be expected to covary with the ECG, we combined these two signals with the EEG channels, conducted principal component analysis (PCA) rather than ICA and removed all components that were dominated by the ECG.

MRI data were preprocessed following the human connectome project preprocessing pipeline (Glasser et al., 2013, 2016). Structural T1 and T2 weighted images were aligned, bias field corrected, skull stripped and nonlinearly registered to MNI space. We applied FreeSurfer's recon-all to reconstruct cortical gray matter surfaces and a subcortical gray matter volume segmentation. Myelin maps across the surface were created by taking the ratio of T1w/T2w from voxel intensities inside the cortical gray matter (Glasser & Van Essen, 2011). The first five fMRI scans were removed, and motion correction was performed by aligning the first image to the series. In this stage we also checked for potential scanner artifacts due to heating. Motion parameters served as regressors when cleaning the fMRI data from remaining motion-related artifacts via ICA. The fMRI data were corrected for echo-planar imaging distortion using a gradient echo field map, aligned to the T1w image as well as MNI space and bias field corrected. The fMRI data were converted into the CIFTI file format, with time series of voxels inside the cortical gray matter ribbon being mapped onto cortical surface vertices and the subcortical gray matter being resampled onto a standard volume mesh. Next, fMRI data were cleaned using FSL's FIX tool (Griffanti et al., 2014; Salimi-Khorshidi et al., 2014). In brief, using a pre-trained classifier automatically we labeled independent components as either neural activity or artifacts. The artifact components as well as motion parameters served as regressors to remove the corresponding co-variate from the fMRI. Finally, the FIX classifier was trained on hand-labeled data from all the 23 subjects of this study. Subjects' individual cortical surfaces were registered to a parcellation template (Glasser et al., 2016) of the human connectome project following a multimodal surface registration approach (Robinson et al., 2014, 2018). The features used for the surface registration were cortical folding, myelin maps, resting state network locations and visuotopic maps. The pre- and post-task fMRI data were used to identify subject individual resting state network locations and visuotopic maps. Aligned fMRI data entered statistical analysis.

2.4.3 | EEG beamformer analysis

Source localization of the β-rhythm was realized using dynamical imaging of coherent sources beamformers (Gross et al., 2005) with tissue segments (skin, skull, cortical spinal fluid, gray and white matter) determined through finite-element-modeling. For both we employed the open-source Fieldtrip toolbox and used their template MRI (Oostenveld, Fries, Maris, & Schoffelen, 2011).

Beamformers for motor event-related β-power
Upon visual inspection of motor-related potentials, we selected the maximum increase in hand force as central events for the subsequent EEG analysis because the surround epochs reveal the maximum difference between β-synchronization and de-synchronization (Figure 3). Epochs of ±400 ms before and after these events served as contrast for subsequent statistics. To identify significance of beamformer power, we followed a Monte Carlo approach with cluster-based test statistics for both groups (with a significance threshold of $\alpha_{cluster} = 0.01$, Nichols and Holmes (2002)). Cluster-level statistics were determined for the separate groups as the sum of *t*-values per cluster. Probabilities were determined by collecting trials of pre- and post-event intervals and test statistics were computed on randomly chosen partitions. These steps were repeated 8,192 times to construct the permutation density of the test statistics, which allowed for using a dependent samples *t*-test between pre- and post-event epochs (significance threshold $\alpha = 0.05$). Following the same approach
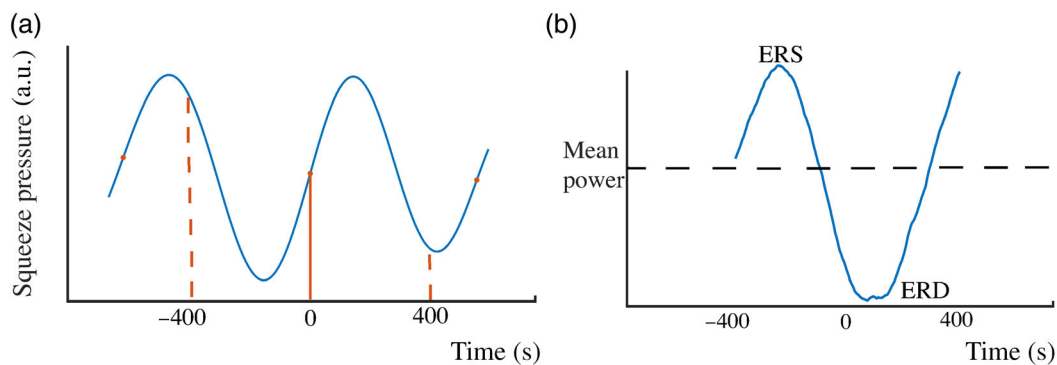
FIGURE 3 Illustration event definition. Left panel: Pressure inside the air-filled rubber bulb; maximum changes of hand force were defined as central events in the motor event-related beamformer approach. Epochs of ±400 ms before and after these events served as contrast. Right panel: Corresponding event-related synchronization (ERS) and desynchronization (ERD) in the β-band of the EEG signal (electrode C3)

but using an independent *t*-test, we tested for significant differences between groups (α < .05). While we focused on β-band activity, we would like to note that we provide all the corresponding findings for the α-frequency band (8–14 Hz) as Supplementary Material S2. Beamformer outcomes were parcellated using the SPM anatomical atlas (Eickhoff et al., 2005). ROIs were defined via significant outcomes of the aforementioned tests and corresponding virtual sensors were defined via the mean spatial filter over each ROIs onto which the EEG data were projected after band-pass filtering in the frequency band under study (β-band in the main text, α-band in Supplementary Material S2). The motor-event-related β-amplitude modulation per trial and for the two resting state blocks (based on randomly placed virtual events) was evaluated as described in Houweling, Beek, and Daffertshofer (2010); see also Neuper, Wörtz, and Pfurtscheller (2006). In a nutshell, we normalized the β-band time-series of the virtual sensor to baseline, that is, the first resting state recording, computed the mean Hilbert amplitude and performed a time-locked averaging (David, Kilner, & Friston, 2006) over the aforementioned ±400 ms epochs. We further evaluated with a generalized estimating equation whether the motor event-related β-modulation correlated with the behavioral performance per trial.

Beamformers for average motor task execution β-power
For both groups we also computed grand-average source-level β-power across learning vs. pre-learning rest, also referred to as task-related power (Andres et al., 1999; Gerloff et al., 1998; Serrien, Cassidy, & Brown, 2003; Toro et al., 1994). With this we tested whether β-power during motor task execution differed between groups, again using a voxel-wise permutation tests with an independent samples *t*-test.

2.4.4 | EEG regressors for analysis with fMRI

We analyzed the fMRI data using general linear modeling (GLM) as outlined below. When combining fMRI with EEG, the source localized EEG served as an additional regressor. For this, we estimated the instantaneous Hilbert amplitude in the frequency-band of interest. For every scan epoch (700 in total) we utilized the mean β-amplitude 800 ms around every motor event and averaged over the events per scan. To accommodate for delays and dispersions in the BOLD-responses, the regressors were convolved with the double gamma hemodynamic response function (HRF) (Grinband, Steffener, Razlighi, & Stern, 2017) using the FMRIB Software Library; see Figure 4.

2.4.5 | fMRI/EEG

Prior to statistical analysis, the fMRI data were spatially smoothed both on the surface and in the subcortical volume using a 4 mm FWHM Gaussian Kernel to suppress spatial noise and to increase the signal-to-noise ratio. To remove low-frequency noise, the data were also filtered with a Gaussian-weighted linear high-pass filter with a cutoff of 135 s. On single-subject level, we fitted the GLM: $Y = \beta_k X_k + \varepsilon$, using the grayordinates-wise BOLD data Y in CIFTI format, that is, the time series from cortical vertices and subcortical voxels (Friston et al., 1995). Here, $\beta_k X_k$ denotes the design matrix and ε the residual error. To build the design matrix we used the task paradigm and combined it with the EEG source-localized β-amplitude (Figure 4, bottom panel). The latter stemmed either from contralateral M1 (left area 4a) or from frontal cortex (left area 6 ∼ premotor area), both according to the SPM atlas (Eickhoff et al., 2005). We contrasted each regressor against baseline and both regressors against each other to estimate statistical effects of interest. When both regressors—task and EEG—are placed in a single GLM, the parameter estimates will reflect the activation in BOLD of one regressor adjusted for the effect of the other. By consequence, the variance explained by both regressors will be removed, isolating the effect of the EEG regressor. Note that by conducting orthogonalization, the shared information of the two regressors is attributed to the regressor that is not orthogonalized (Mumford, Poline, & Poldrack, 2015); hence, orthogonalization was not applied. Based on these single-subject contrasts, a mixed-effects group-level analysis was performed using a paired or unpaired two

FIGURE 4 Computation of the regressors. Illustration of the computation of the beta amplitude and the resulting regressors. From the source-localized EEG (top panel), the Hilbert amplitude was determined and the mean β-amplitude 800 ms around the motor events was averaged for every scan (middle panel, blue) and convolved with the hemodynamic response function (HRF) to determine the HRF-convolved regressor (bottom panel, blue). The red curves show the regressor of the task design (in the bottom panel after HRF-convolution)
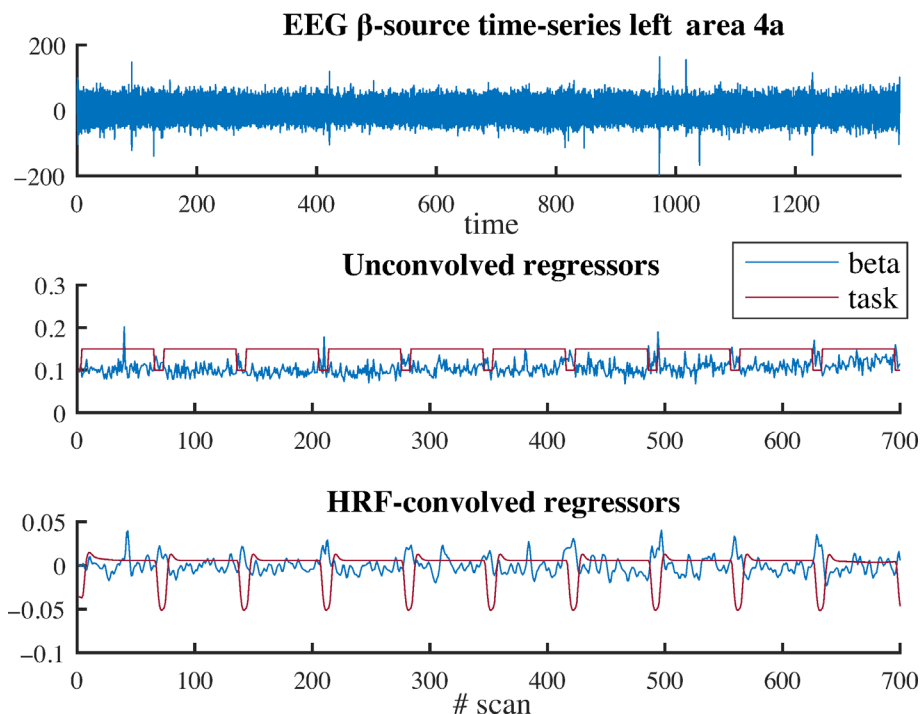
group *t*-test, to contrast within- and between-group activation, respectively. The latter contrasts were masked to reveal only those areas that deemed significant using the single-group activation contrast. Finally, we thresholded the statistical maps using a false discovery rate of $q = 0.01$ (Genovese, Lazar, & Nichols, 2002).

3 | RESULTS

EEG data of nine participants (five young, four older) had to be excluded due to technical errors during acquisition. In seven of these cases, the EEG's DAC experienced a buffer overflow in the local stack, one participant's fMRI volumes were not properly stored, and one participant's BOLD data could not be pre-processed because the segmentation of brain and non-brain tissue appeared incorrect. Two participants showed extensive head motion and had to be excluded from further fMRI analysis. Another two showed clear deviations in motor behavior and were considered outliers. Data of 27 participants entered behavioral, EEG and fMRI analysis.

3.1 | Motor behavior

Since the assumption of sphericity was violated for the frequency locking values per trial in both groups ($\chi^2[44] = 83.43$, $p < .001$), we corrected the degrees-of-freedom ($\varepsilon = .564$). We found significant main effects for Trial and Age ($F(5.08,126.99) = 3.621$, $p < .01$, $\eta_p^2 = .127$ and $F(1,25) = 11.723$, $p < .01$, $\eta_p^2 = .319$, respectively) but could not establish a significant Age × Trial interaction ($p = .142$). The performance level during the first trial was significantly lower in the older than in

the younger participants ($p < .05$, $d = 1.406$). This difference did not persist in the last trial but re-appeared during retention testing.

Post hoc *t*-tests revealed an improved performance during trial 10 when compared to trial 1 in the older ($p = .004$, $d = 1.045$) but not for the younger group ($p = .072$). Both groups showed significant differences between the first trial and the retention test (young: $p < .05$, $d = .807$, older: $p < .01$, $d = .992$), while we could not establish any significant differences between the last trial and the retention test ($p > .05$). This suggests that practicing culminated in proper motor learning (Figure 5).
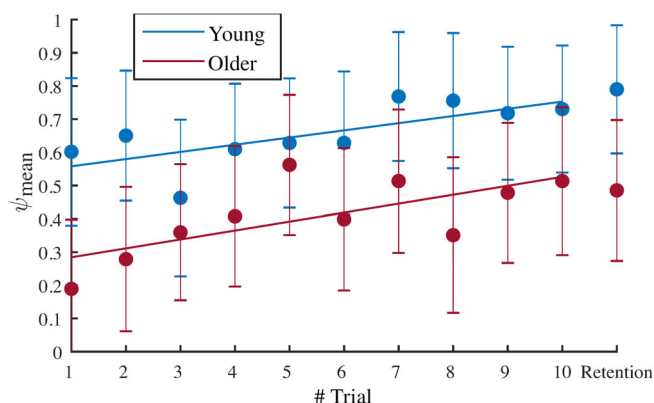

FIGURE 5 Behavioral results. Mean performance and standard error per trial for 13 younger (blue) and 14 older (red) participants during the fMRI/EEG recordings and the mean performance and standard error of the retention test. The regression lines have been added to ease visualization

3.2 | EEG

As summarized in Figure 6, the β-band power that contrasted ±400 ms pre- and post-motor event displayed significant motor-task positive modulation (i.e., an increase during the motor event) that was lateralized in both groups. Differences between groups over the complete task were not significant. We used left Brodmann's area 4a, that is, M1 contralateral to the force producing hand, as ROI for subsequent analyses (younger: $t = -6.94$, older: $t = -3.73$).

For both groups, we found motor-event-related β-amplitude modulations in contralateral M1. This was more pronounced in the younger group (Figure 7). The correlations between motor-task related modulation and behavioral performance per trial did not reach significance (young: $r = .387$, $p = .269$; older: $r = .241$ $p = .502$). The standard deviations (Figure 7 in light blue for the younger and light red for older group) indicated a substantial intra-group variability, which arguably caused the absence of significant differences for this event-related modulation. We would like to note that when not normalizing the β-amplitudes to their average values during the first baseline resting state recording, an on average lower beta amplitude could be identified in the older participants (Figure 7b). This observation does agree with the group differences shown in Figure 8: the younger group displayed a less strong decrease in β-power in bilateral PM1 than the older group, with a peak t-value of 4.14 ($p < .05$, $d = .489$) in left area 6 (premotor area). Further task-vs.-rest descriptive statistics of β-power for both age groups separately can be found in Supplementary Material S3.

3.3 | fMRI

We observed significant task-induced BOLD signal modulations in visual and motor regions both in younger and older participants (FDR corrected $p < .01$). As expected, the right-hand motor task was primarily accompanied with activity in left M1. We also found task-related activity in left and right PM1 in both groups and in SMA in the younger participants (Figure 9). Subcortical areas were active that are known for being involved in regulating movement and motor learning, including putamen, thalamus, and cerebellum.

To identify brain areas with task-related deactivation, we used the task design as regressor, yielding patterns in both groups that largely resemble the default mode network (DMN, see Figure 10). According to Andrews-Hanna, Smallwood, and Spreng (2014), the DMN consists of the posterior and anterior cortical midline structures, with hubs located in the posterior cingulate cortex and precuneus, the medial prefrontal and the parietal cortex (Brodmann areas 7 and 39/40). Neither in task positive nor in task negative BOLD responses we found significant younger/older group difference during motor learning.

3.4 | fMRI/EEG

Since the EEG beamformer results revealed left M1 as main ROI, we employed the corresponding β-amplitudes to define supplementary regressors. For both groups, the regions that significantly correlated positively with the β-amplitude regressor were primary motor- and visual cortex, Brodmann area 9, 39, and 32, putamen and hippocampus. The activated Brodmann's areas are considered to contribute to short-term memory and attention (Figure 11). For the older adults also the primary somatosensory cortex, insula, thalamus, and amygdala came significantly to the fore. A remarkable difference in comparison to the task-correlated fMRI patterns was a positive correlation in the right (ipsilateral) M1 present both
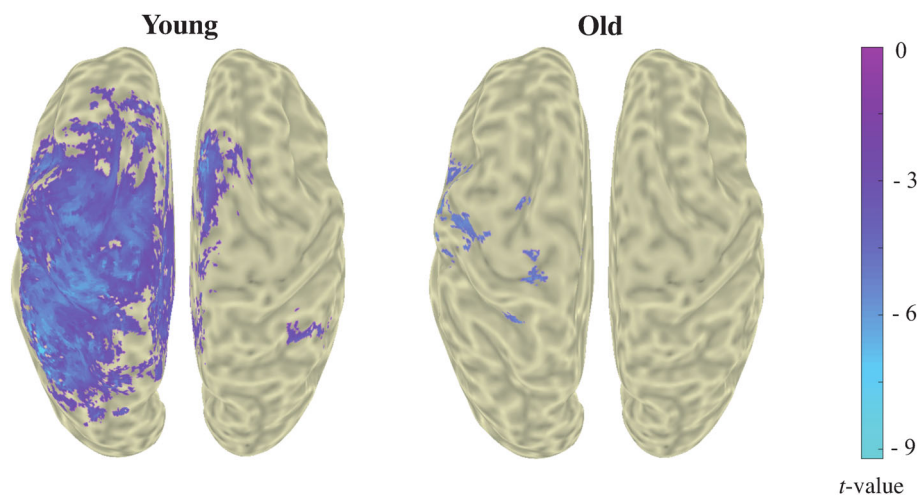

FIGURE 6 Contrast of β-power between pre- and post-motor event. Adaptive spatial filtering identified cortical sources when contrasting the β-band power over the 400 ms before the event vs. the β-band power ± 400 ms after the event. Grand averages shown correspond to younger and older participants ($N = 13$ and $N = 14$, respectively). Permutation tests with a dependent samples t-statistic revealed voxels comprising significant differences between ±400 ms pre- and post-motor event for both younger and older groups. Colors represent t-values masked with a threshold of $p < .05$. Based on this result left area 4a (M1) was included as ROI for analysis

FIGURE 7 (a) Learning block-wise event-related β-amplitudes in contralateral (left) M1. Grand average of event-related amplitudes in left M1 (Broadman area 4a) for pre- and post-rest and 10 task blocks for the younger and older groups (upper row in blue, N = 13 and lower row in red, N = 14, respectively) group; amplitudes (in arbitrary units, including standard deviations [transparent], and standard errors of the mean) are normalized to the mean β-amplitude value of the first resting state trial (baseline). (b) Non-normalized event-related β-amplitudes in contralateral (left) M1. Grand average of event-related amplitudes in left M1 for pre- and post-rest and 10 task blocks for the younger and the older group (blue and red, respectively); amplitude, standard deviations (transparent), and standard errors of the mean are displayed in arbitrary units—compare with (a) that contains the normalized amplitudes. The green line has been added to ease visual inspection
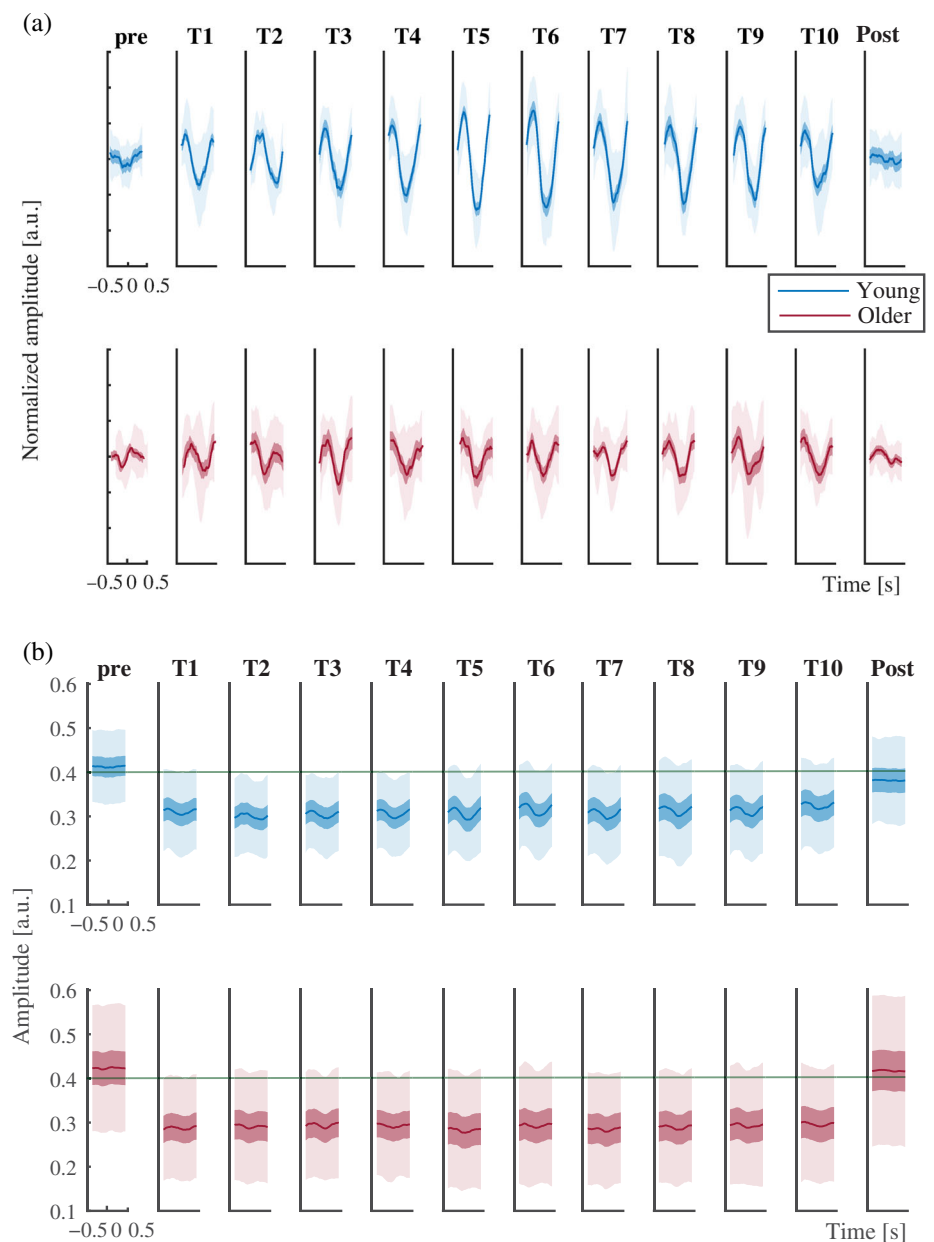
groups. Moreover, bilateral premotor areas, the anterior intraparietal area and some visual areas showed a significant negative correlation when including the β-amplitude regressor (Figure 12). The older group showed a negative correlation between fMRI-BOLD and β-amplitude in M1 in a small part of left M1. Again, we could not establish any significant group differences.

Since we did find a significant group difference (younger > old) in the mean β-power, where Brodmann's area 6 turned out to be the most significant ROI (Figure 8), we used the corresponding source-reconstructed β-amplitude as regressor for the BOLD analysis. This revealed regions like the ones when using the β-amplitude in left M1, though here the regions appeared more focal (Figure 13 and 14). Still, group differences in fMRI-BOLD could not be established.

4 | DISCUSSION

We simultaneously acquired EEG and fMRI-BOLD signals in younger and older participants when learning a unimanual motor task in the presence of visual feedback. The experiment was designed to unravel aging-related differences in visuomotor coordination learning. Both age groups improved performance due to learning. The training was accompanied by task-related changes in the motor event-related EEG β-power (Figure 6) and in the mean β-power during motor execution (Figure 8). The latter differed significantly between groups in premotor areas. The fMRI-BOLD also displayed significant changes during motor learning, but in contrast to the EEG and against our expectation the two groups did not differ significantly.

Our behavioral outcomes revealed that both groups were able to learn the motor task to a similar degree. Yet, there was an offset at

baseline, that is, prior to starting to learn, which implies poorer performance in the older group that persisted throughout the learning. When correcting for this by stratifying the starting performance level, the rate of learning largely agreed between groups in line with earlier findings (Bhakuni & Mutha, 2015; Hoff et al., 2015). The 24-hours follow-up retention test confirmed motor learning in both groups rather than mere training effects. As expected also during the retention test, we observed decrease in motor performance with increasing

age (Houx & Jolles, 1993; Kauranen & Vanharanta, 1996; Shimoyama et al., 1990; Smith et al., 1999; Ward & Frackowiak, 2003).

The β-band beamformers were signified by activity in left M1, that is, contralateral to the force producing hand. While this was the case in both groups, lateralization appeared more pronounced in the younger group. In fact, we did expect to find less lateralized activity in the older adults than in the younger ones (Cabeza, 2001). It seems that aging limits the deactivation of ipsilateral M1 during unimanual movement. By hypothesis this is because of a reduced increase in intra-hemispheric inhibition and compromised phase locking between premotor and primary motor areas (Coxon et al., 2010; Daffertshofer et al., 2005; Goble et al., 2010; Hinder et al., 2012; Van Impe et al., 2009; van Wijk et al., 2012). Yet, we could not confirm this as ipsilateral activity did not reach statistical significance in either group. Interestingly, however, Larivière et al. (2019) reported aging-related difference during a unimanual isometric handgrip task. In this more recent MEG study, participants produced similar levels of activity irrespective of age, but older participants displayed sharp activation peaks which led the authors speculate about greater temporal synchrony in synaptic input to cortical pyramidal neurons in the older group (Sherman et al., 2016).

We found significant differences between the groups in mean β-power during motor task execution located in (bilateral) premotor areas. The average β-power during motor execution in the younger participants was substantially elevated. An overall decrease in β-power when contrasting motor tasks with rest has been well described in M/EEG research, where also coherence between bilateral premotor and sensorimotor areas appears to increase (Calmels et al., 2006; Calmels, Hars, Holmes, Jarry, & Stam, 2008; Farber & Anisimova, 2000; Ford, Goethe, & Dekker, 1986; Gerloff et al., 1998; Lange, Braun, & Godde, 2006; Man'kovskaya, 2006; Manganotti et al., 1998; Mima, Matsuoka, & Hallett, 2000; Serrien, 2008; Shibata et al., 1998; Svoboda, Sovka, & Stancak, 2002; van Wijk et al., 2012;
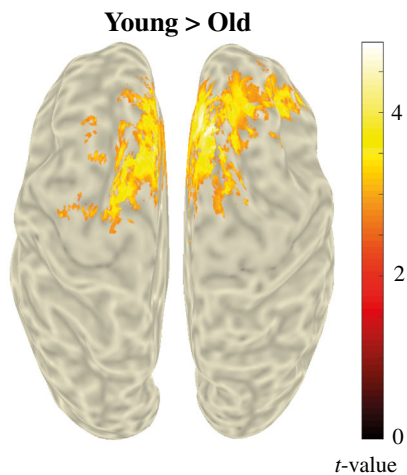

FIGURE 8 Group differences of the β-power averaged over motor execution. Permutation tests with an independent samples t-statistic revealed significant β-power differences during learning between younger and older groups. Colors represent t-values, masked with a threshold of p < .05. Based on this result left area 6 (PM1) was included as ROI for analysis
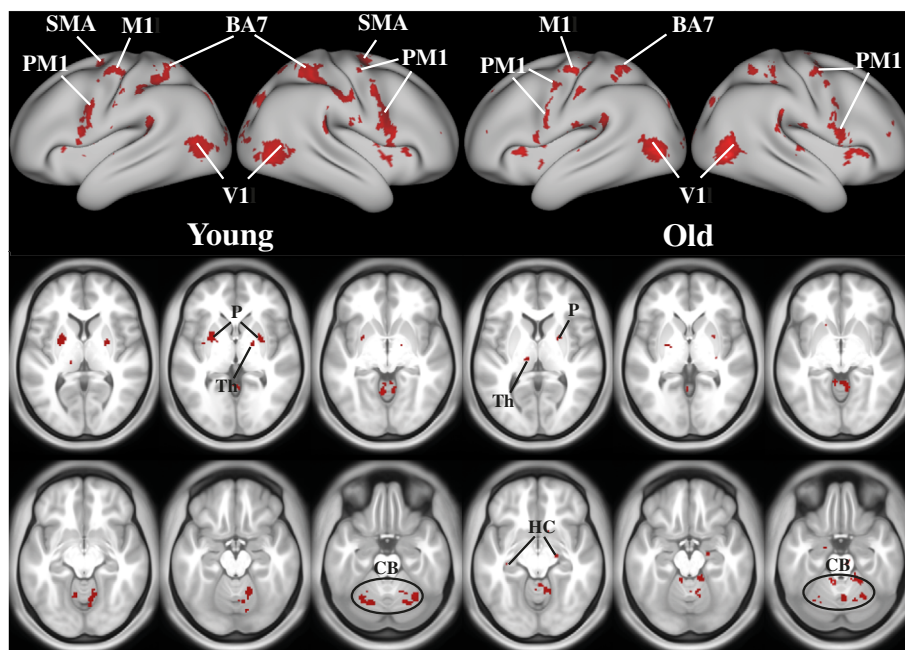

FIGURE 9 Task-positive BOLD responses. Using the task design as regressor, we identified significant clusters of task positive BOLD responses displayed in red (unpaired two group t-test, FDR-corrected p < .01). We used the Glasser parcellated brain template to display the BOLD patterns. PM1, premotor cortex; M1, motor cortex; SMA, supplementary motor cortex; BA7, Brodmann area 7; V1, visual cortex; P, putamen; CB, cerebellum; Th, thalamus

FIGURE 10 Task-negative BOLD responses. The task design as regressor revealed regions that significantly deactivated in blue (unpaired two group *t*-test, FDR-corrected *p* < .01). BA7/8/39/40, Brodmann area 7/8/39/40; PF, prefrontal cortex; STS, superior temporal sulcus; PCC, posterior cingulate cortex; V1, visual cortex; CB, cerebellum; Th, thalamus; vDC, ventral diencephalon
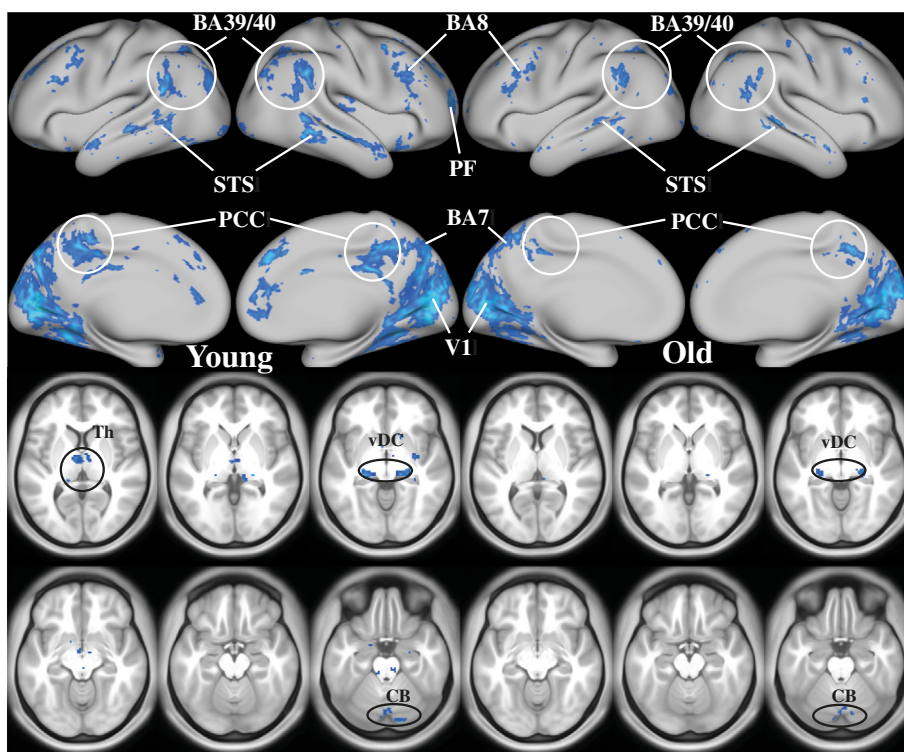

FIGURE 11 BOLD responses when including β-amplitudes in left M1 as additional regressor. Using both the task design and motor-related β-amplitudes in left M1 as regressors, we evaluated regions that significantly correlated with these regressors in red (unpaired two group *t*-test, FDR-corrected *p* < .05). M1, motor cortex; S1, somatosensory cortex; BA9/32/39, Brodmann area 9/32/39; V1, visual cortex; P, putamen; CB, cerebellum; Th, thalamus; AM, amygdala; HC, hippocampus
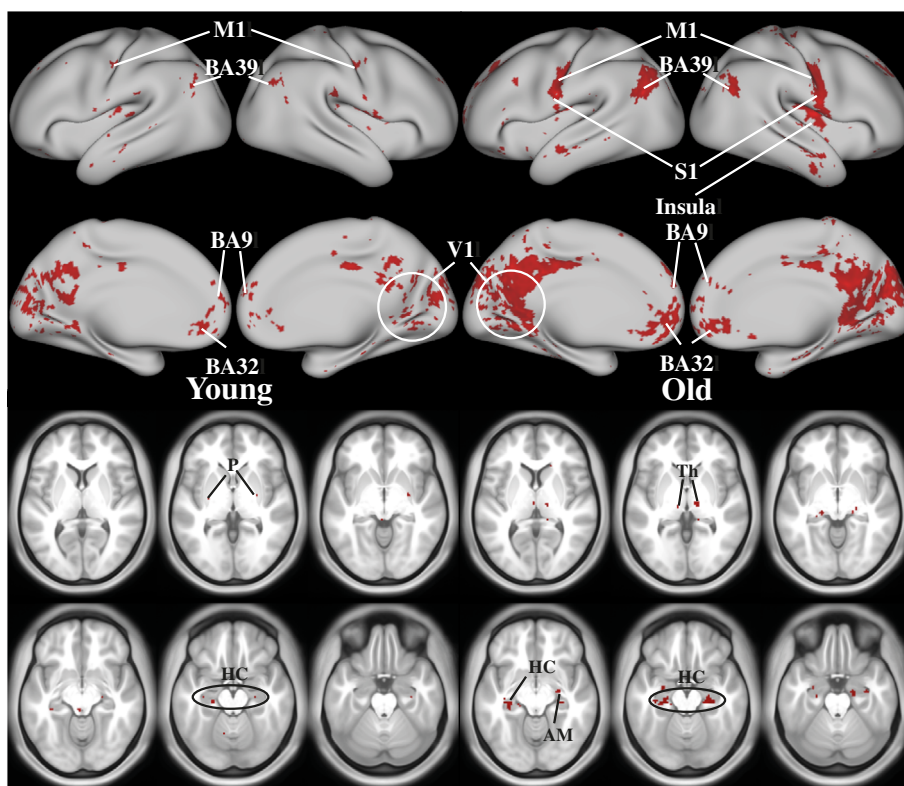
Vecchio et al., 2014; Wang et al., 2017). Our results show that the drop in β-power is significantly greater in older compared to younger adults, with premotor areas as main region with age-related differences. This agrees with Espenhahn et al. (2019), who showed that magnitude of movement-related β-desynchronization to be affected by age. In their study, older subjects displayed a greater β-power decrease in both sensorimotor cortices during the movement than their younger counterparts.
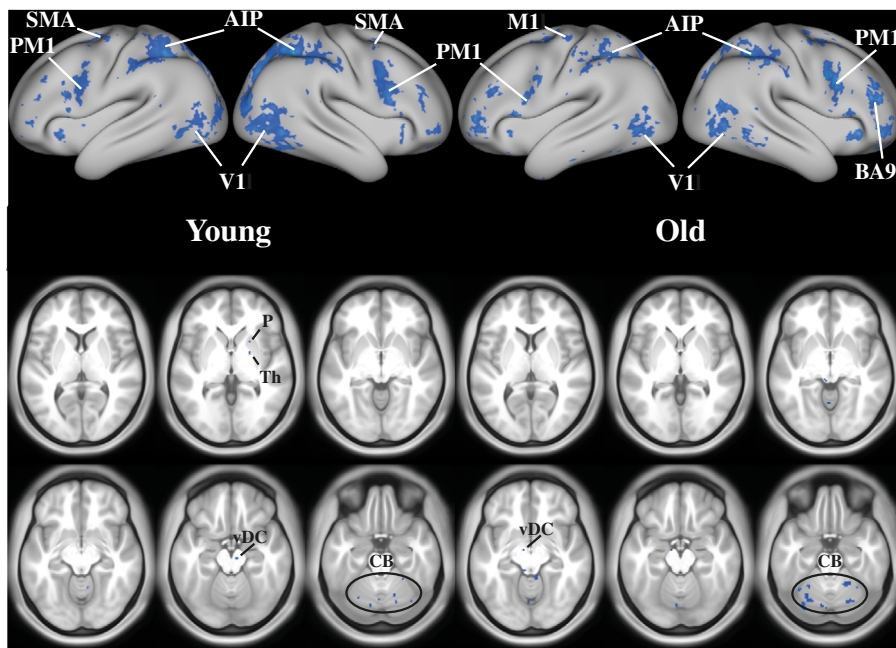
FIGURE 12 Negative fMRI-BOLD signal correlates of β-amplitude in left M1. Regions that significantly correlated negatively are indicated in blue (unpaired two group t-test, FDR-corrected p < .05). PM1, premotor cortex; M1, motor cortex; AIP, anterior intraparietal area; SMA, supplementary motor cortex; BA9, Brodmann area 9; V1, visual cortex; CB, cerebellum; Th, thalamus; vDC, ventral diencephalon
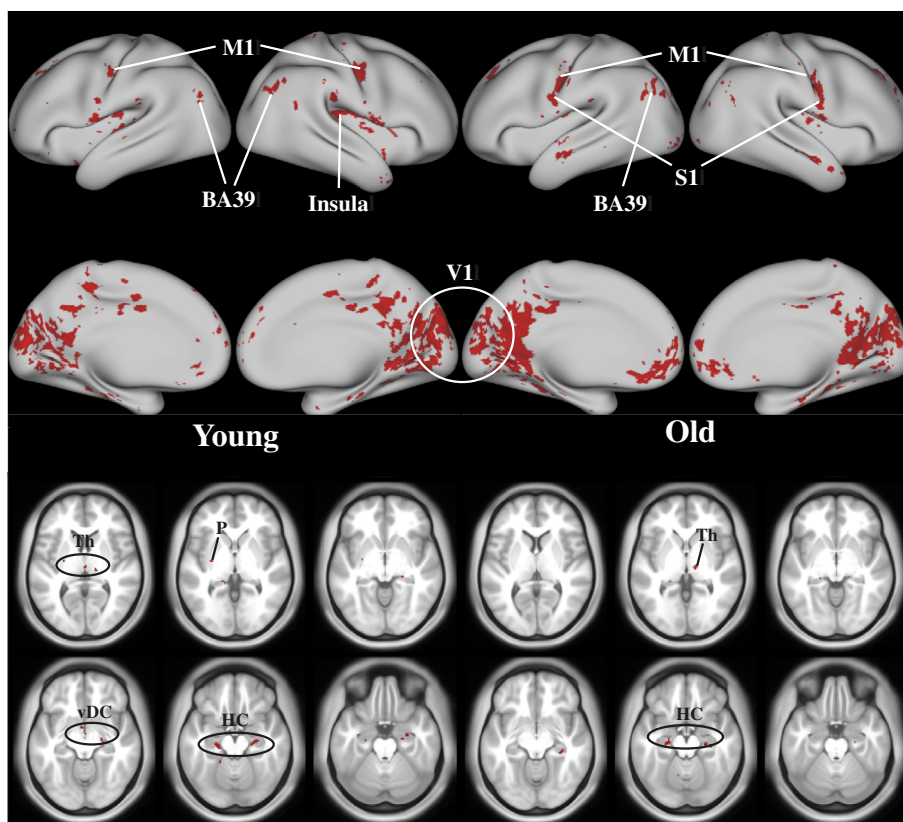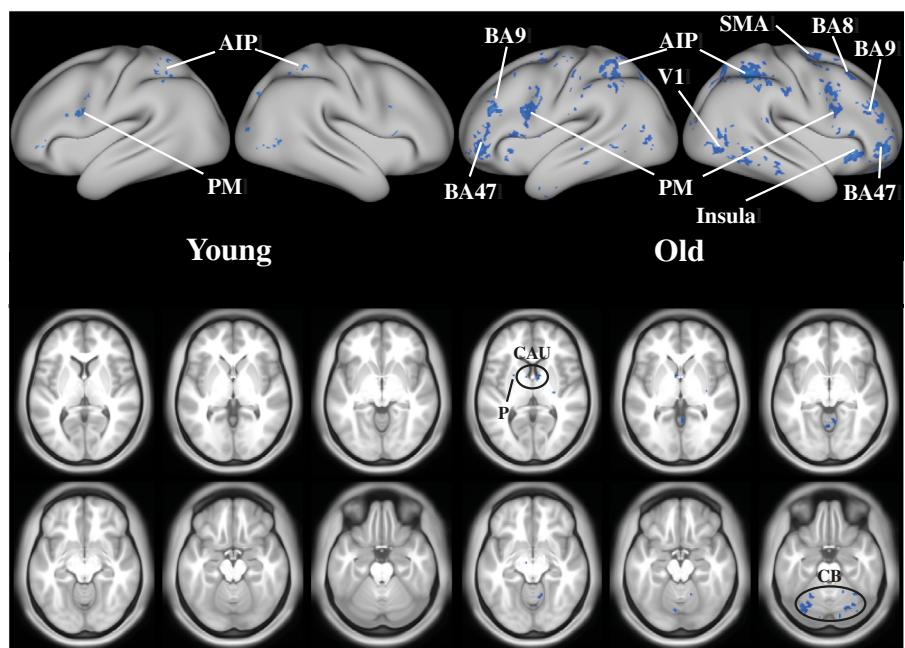

FIGURE 13 BOLD responses based on β-amplitude in left PM1 (area 6) as supplementary regressor. With task design and the motor-related β-amplitudes in left area 6 (left PM) as regressor, we found several regions that significantly correlated in red (unpaired two group t-test, FDR-corrected p < .05): M1, motor cortex; S1, somatosensory cortex; BA39, Brodmann area 39; V1, visual cortex; P, putamen; Th, thalamus; vDC, ventral diencephalon; HC, hippocampus

The fMRI-BOLD patterns contained significant task-related activation also in left M1, in bilateral PM1, SMA and visual areas, while the deactivation patterns largely agreed with the DMN. None of these differed significantly between age groups. The lack of aging-effects in fMRI-BOLD persisted despite supplementing analysis by EEG-based regressors. This was even the case when the regressor was used that did reveal such differences when analyzing EEG alone. Next to left M1, when using these EEG-based regressors we also found positive correlations between source-reconstructed β-amplitudes in right M1, that is, ipsilateral to the force producing hand. This was the case in both groups and does suggest the involvement of an ipsilateral controller in our unimanual perceptual motor task. Remarkably, the older

group also showed a negative correlation between the β-amplitude regressor and a small part of the left M1. And there were significant negative BOLD/β-amplitude correlations in both groups as well as in the anterior intraparietal area and some visual areas—recall that we used visual feedback to facilitate motor learning. More importantly, these correlations were also visible in bilateral PM1, at least when combining fMRI and EEG.

When combining fMRI and EEG we could identify positive and negative correlations in relevant motor areas during this unimanual motor task in both groups. To what extent this really confirms the idea of effective interhemispheric inhibition that we outlined in Section 1 remains a puzzle. As discussed in Chettouf et al. (2020), direction and location of both inhibition and excitation, that is, which region inhibits or excites appears to depend on the motor task that is performed. More precisely it depends on the degree of task difficulty, even if it comes to inhibiting or exciting M1 during a unimanual task. As such it could well be that the direction of correlation (positive or negative) may differ because groups differ in the degree of experienced task difficulty. The puzzle really starts when recalling that this task difficulty changes as a function of motor learning. However, we prefer to abstain from digging deeper in these speculative ideas.

We expected that interactions through the CC would be altered with age leading to an imbalance of the effective interhemispheric inhibition. Yet, we did not find any significant age-related differences in the combined EEG-fMRI analysis. This might be due to a small sample size per group (N = 13 vs. 14). On the other hand, we did find significant differences in EEG (Figure 8). This suggests that—in principle—our sample size sufficed to identify (electro-)physiological differences but the metabolic changes—if present—came with very small effect sizes. EEG reflects the degree of synchronization/desynchronization of pyramidal cell membrane potential oscillations that often is associated with changes of local firing rates and synaptic

activity (Schirner, McIntosh, Jirsa, Deco, & Ritter, 2018), yet a generic link with to the BOLD signal is still lacking (Raichle, 2001). While limited statistical power might be a reason for the absence of group differences of the combined EEG-fMRI analysis—and so might be atrophic differences that we did not assess—it might also be conceivable that correlates of EEG in fMRI remain the same across age groups. For the EEG regressor, we utilized the mean β-amplitude 400 ms around the motor event, which is slightly different from our event-related analysis where we contrasted pre and post epochs. This was motivated by the clear difference in average β-power during motor execution between groups though this was most pronounced in premotor areas.

A recent study with a similar design revealed very comparable behavioral results: a visuomotor tracking skill was learned to similar extent in both younger and older adults (no interaction effect), while motor performance was lower in the older compared to the younger (Berghuis et al., 2019). There older adults display stronger fMRI-BOLD activation. While this seemingly contradicts our findings, one should note that when Berghuis et al. (2019) added the whole-brain gray matter volume a covariate to their model, the observed differences between younger and older adults were no longer significant. Apparently, differences in gray matter "explained" the age-related differences that were found.

Both groups showed a similar decrease of brain activation over time (from pre- to post-test), showing that the visual processing areas are more involved when performing the task for the first time compared to immediately after the training session—apparently our participants had to rely more on the visual feedback when new to the motor task and did require less of it in the course of learning. Yet, changes in brain-deactivations were age-dependent in specific areas that are part of the DMN (Raichle, 2015). This agrees with the idea that DMN modulation is "dysregulated"; with increasing age (Park & Reuter-Lorenz, 2009) and suggests the employment of compensatory

mechanisms by older adults to achieve similar learning rates as younger ones.

As said, we facilitated learning by providing a "simple" perceptual goal (Mechsner et al., 2001). Put differently, the task under study was a perceptual-motor task with substantial involvement of visual areas (see above). As such we must admit that our findings may not reflect "pure" motor behavior but also contain the integration of—in our case—visual information. One should realize, however, that "pure" motor behavior hardly exists as, under normal circumstance, motor control always includes the processing of some form of sensory information.

As another limitation we should note that we incorporated a template anatomical MRI. Reason for this was that our experimental setting did not allow for co-registering the precise location of the EEG electrodes though this is known to largely improve spatial accuracy (Michel & Brunet, 2019; Shirazi & Huang, 2019). Our source localization has certainly room for improvement keeping in mind that our "clinical" EEG-setting will always come with limited spatial resolution (Kalogianni et al., 2018).

Our present data support the pivotal role of oscillatory activity in premotor areas during motor coordination in line with the model shown in Figure 1. The EEG finding support the idea that this role changes as a function of age: A stronger PM1 β-rhythm desynchronization in older adults makes the ipsilateral PM1 → M1 inhibition less effective which arguably causes poorer motor performance with increasing age.

5 | CONCLUSION

Demanding sensorimotor coordination performance that improves with learning is diminished in the older adults. We found β-power in the premotor areas during learning to be weaker in older than in younger adults. That is, task-related β-desynchronization becomes less pronounced. Irrespective of age the β-activity correlates negatively with fMRI in PM1 and positively in M1. Despite that lack of clear-cut age group differences in the fMRI even when combined with EEG as a regressor, the EEG-results alone let us advocate a decreased PM1-mediated intra-hemispheric inhibition of M1 in older adults to be a potential source for elevated interhemispheric crosstalk and diminished motor performance at increased age.

CONFLICT OF INTEREST

None.

DATA AVAILABILITY STATEMENT

The data that support the findings of this study are available from the corresponding author upon reasonable request.

ORCID

Sabrina Chettouf https://orcid.org/0000-0001-6773-9035
Andreas Daffertshofer https://orcid.org/0000-0001-9107-3552

REFERENCES

Anami, K., Mori, T., Tanaka, F., Kawagoe, Y., Okamoto, J., Yarita, M., ... Saitoh, O. (2003). Stepping stone sampling for retrieving artifact-free electroencephalogram during functional magnetic resonance imaging. *NeuroImage*, *19*(2), 281–295.

Andres, F. G., Mima, T., Schulman, A. E., Dichgans, J., Hallett, M., & Gerloff, C. (1999). Functional coupling of human cortical sensorimotor areas during bimanual skill acquisition. *Brain*, *122*(Pt 5), 855–870.

Andrews-Hanna, J. R., Smallwood, J., & Spreng, R. N. (2014). The default network and self-generated thought: Component processes, dynamic control, and clinical relevance. *Annals of the new York Academy of Sciences*, *1316*(1), 29–52.

Berghuis, K. M., Fagioli, S., Maurits, N. M., Zijdewind, I., Marsman, J.-B. C., Hortobágyi, T., ... Bozzali, M. (2019). Age-related changes in brain deactivation but not in activation after motor learning. *NeuroImage*, *186*, 358–368.

Bhakuni, R., & Mutha, P. (2015). Learning of bimanual motor sequences in normal aging. *Frontiers in Aging Neuroscience*, *7*, 76.

Boonstra, T. W., Daffertshofer, A., Breakspear, M., & Beek, P. J. (2007). Multivariate time–frequency analysis of electromagnetic brain activity during bimanual motor learning. *NeuroImage*, *36*(2), 370–377.

Cabeza, R. (2001). Cognitive neuroscience of aging: Contributions of functional neuroimaging. *Scandinavian Journal of Psychology*, *42*(3), 277–286.

Calmels, C., Hars, M., Holmes, P., Jarry, G., & Stam, C. J. (2008). Non-linear EEG synchronization during observation and execution of simple and complex sequential finger movements. *Experimental Brain Research*, *190*(4), 389–400. https://doi.org/10.1007/s00221-008-1480-z

Calmels, C., Holmes, P., Jarry, G., Hars, M., Lopez, E., Paillard, A., & Stam, C. J. (2006). Variability of EEG synchronization prior to and during observation and execution of a sequential finger movement. *Human Brain Mapping*, *27*(3), 251–266.

Carson, R. (2005). Neural pathways mediating bilateral interactions between the upper limbs. *Brain Research Reviews*, *49*(3), 641–662.

Carson, R. G. (2020). Inter-hemispheric inhibition sculpts the output of neural circuits by co-opting the two cerebral hemispheres. *The Journal of Physiology*, *598*(21), 4781–4802.

Chettouf, S., Rueda-Delgado, L. M., de Vries, R., Ritter, P., & Daffertshofer, A. (2020). Are unimanual movements bilateral? *Neuroscience & Biobehavioral Reviews*, *113*, 39–50.

Coxon, J. P., Goble, D. J., Van Impe, A., De Vos, J., Wenderoth, N., & Swinnen, S. P. (2010). Reduced basal ganglia function when elderly switch between coordinated movement patterns. *Cerebral Cortex*, *20*(10), 2368–2379.

Daffertshofer, A., Peper, C., & Beek, P. (2000). Spectral analyses of event-related encephalographic signals. *Physics Letters A*, *266*(4–6), 290–302. https://doi.org/10.1016/S0375-9601(99)00908-1

Daffertshofer, A., Peper, C. L., & Beek, P. J. (2005). Stabilization of bimanual coordination due to active interhemispheric inhibition: A dynamical account. *Biological Cybernetics*, *92*(2), 101–109. https://doi.org/10.1007/s00422-004-0539-6

David, O., Kilner, J. M., & Friston, K. J. (2006). Mechanisms of evoked and induced responses in MEG/EEG. *NeuroImage*, *31*(4), 1580–1591.

Eickhoff, S. B., Stephan, K. E., Mohlberg, H., Grefkes, C., Fink, G. R., Amunts, K., & Zilles, K. (2005). A new SPM toolbox for combining probabilistic cytoarchitectonic maps and functional imaging data. *NeuroImage*, *25*(4), 1325–1335.

Espenhahn, S., van Wijk, B. C., Rossiter, H. E., de Berker, A. O., Redman, N. D., Rondina, J., ... Ward, N. S. (2019). Cortical beta oscillations are associated with motor performance following visuomotor learning. *NeuroImage*, *195*, 340–353.

Farber, D. A., & Anisimova, I. O. (2000). Functional organization of the cortex of the large hemispheres during voluntary movement performance: Age aspect. *Human Physiology*, *26*(5), 537–544. https://doi.org/10.1007/BF02760369

Fischl, B. (2012). FreeSurfer. *Neuroimage*, *62*(2), 774–781.

Ford, M. R., Goethe, J. W., & Dekker, D. K. (1986). EEG coherence and power changes during a continuous movement task. *International Journal of Psychophysiology*, *4*(2), 99–110.

Frederiksen, K. S., & Waldemar, G. (2012). Corpus callosum in aging and neurodegenerative diseases. *Neurodegenerative Disease Management*, *2*(5), 493–502. https://doi.org/10.2217/nmt.12.52

Freyer, F., Becker, R., Anami, K., Curio, G., Villringer, A., & Ritter, P. (2009). Ultrahigh-frequency EEG during fMRI: Pushing the limits of imaging-artifact correction. *NeuroImage*, *48*(1), 94–108.

Friston, K. J., Ashburner, J., Frith, C. D., Poline, J. B., Heather, J. D., & Frackowiak, R. S. (1995). Spatial registration and normalization of images. *Human Brain Mapping*, *3*(3), 165–189.

Fujiyama, H., Van Soom, J., Rens, G., Gooijers, J., Leunissen, I., Levin, O., & Swinnen, S. P. (2016). Age-related changes in frontal network structural and functional connectivity in relation to bimanual movement control. *The Journal of Neuroscience*, *36*(6), 1808–1822. https://doi.org/10.1523/jneurosci.3355-15.2016

Genovese, C. R., Lazar, N. A., & Nichols, T. (2002). Thresholding of statistical maps in functional neuroimaging using the false discovery rate. *NeuroImage*, *15*(4), 870–878.

Gerloff, C., Richard, J., Hadley, J., Schulman, A. E., Honda, M., & Hallett, M. (1998). Functional coupling and regional activation of human cortical motor areas during simple, internally paced and externally paced finger movements. *Brain*, *121*(Pt 8), 1513–1531.

Ghacibeh, G. A., Mirpuri, R., Drago, V., Jeong, Y., Heilman, K. M., & Triggs, W. J. (2007). Ipsilateral motor activation during unimanual and bimanual motor tasks. *Clinical Neurophysiology*, *118*(2), 325–332. https://doi.org/10.1016/j.clinph.2006.10.003

Glasser, M. F., Coalson, T. S., Robinson, E. C., Hacker, C. D., Harwell, J., Yacoub, E., ... Jenkinson, M. (2016). A multi-modal parcellation of human cerebral cortex. *Nature*, *536*(7615), 171–178.

Glasser, M. F., Sotiropoulos, S. N., Wilson, J. A., Coalson, T. S., Fischl, B., Andersson, J. L., ... Polimeni, J. R. (2013). The minimal preprocessing pipelines for the human connectome project. *NeuroImage*, *80*, 105–124.

Glasser, M. F., & Van Essen, D. C. (2011). Mapping human cortical areas in vivo based on myelin content as revealed by T1-and T2-weighted MRI. *Journal of Neuroscience*, *31*(32), 11597–11616. https://doi.org/10.1523/JNEUROSCI.2180-11.2011

Goble, D. J., Coxon, J. P., Van Impe, A., De Vos, J., Wenderoth, N., & Swinnen, S. P. (2010). The neural control of bimanual movements in the elderly: Brain regions exhibiting age-related increases in activity, frequency-induced neural modulation, and task-specific compensatory recruitment. *Human Brain Mapping*, *31*(8), 1281–1295.

Griffanti, L., Salimi-Khorshidi, G., Beckmann, C. F., Auerbach, E. J., Douaud, G., Sexton, C. E., ... Mackay, C. E. (2014). ICA-based artefact removal and accelerated fMRI acquisition for improved resting state network imaging. *NeuroImage*, *95*, 232–247.

Grinband, J., Steffener, J., Razlighi, Q. R., & Stern, Y. (2017). BOLD neurovascular coupling does not change significantly with normal aging. *Human Brain Mapping*, *38*(7), 3538–3551.

Gross, J., Pollok, B., Dirks, M., Timmermann, L., Butz, M., & Schnitzler, A. (2005). Task-dependent oscillations during unimanual and bimanual movements in the human primary motor cortex and SMA studied with magnetoencephalography. *NeuroImage*, *26*(1), 91–98.

Hinder, M. R., Fujiyama, H., & Summers, J. J. (2012). Premotor-motor interhemispheric inhibition is released during movement initiation in older but not young adults. *PLoS One*, *7*(12), e52573. https://doi.org/10.1371/journal.pone.0052573

Hoff, M., Trapp, S., Kaminski, E., Sehm, B., Steele, C. J., Villringer, A., & Ragert, P. (2015). Switching between hands in a serial reaction time task: a comparison between young and old adults. *Frontiers in Aging Neuroscience*, *7*, 176.

Holtrop, J. L., Loucks, T. M., Sosnoff, J. J., & Sutton, B. P. (2014). Investigating age-related changes in fine motor control across different effectors and the impact of white matter integrity. *NeuroImage*, *96*, 81–87.

Houweling, S., Beek, P. J., & Daffertshofer, A. (2010). Spectral changes of interhemispheric crosstalk during movement instabilities. *Cerebral Cortex*, *20*(11), 2605–2613. https://doi.org/10.1093/cercor/bhq008

Houweling, S., Daffertshofer, A., van Dijk, B. W., & Beek, P. J. (2008). Neural changes induced by learning a challenging perceptual-motor task. *NeuroImage*, *41*(4), 1395–1407.

Houweling, S., van Dijk, B. W., Beek, P. J., & Daffertshofer, A. (2010). Cortico-spinal synchronization reflects changes in performance when learning a complex bimanual task. *NeuroImage*, *49*(4), 3269–3275.

Houx, P. J., & Jolles, J. (1993). Age-related decline of psychomotor speed: Effects of age, brain health, sex, and education. *Perceptual and Motor Skills*, *76*(1), 195–211.

Hughes, C. M., & Franz, E. A. (2007). Experience-dependent effects in unimanual and bimanual reaction time tasks in musicians. *Journal of Motor Behavior*, *39*(1), 3–8. https://doi.org/10.3200/jmbr.39.1.3-8

Hutchinson, S., Kobayashi, M., Horkan, C., Pascual-Leone, A., Alexander, M., & Schlaug, G. (2002). Age-related differences in movement representation. *NeuroImage*, *17*(4), 1720–1728.

Hyvarinen, A. (1999). Fast and robust fixed-point algorithms for independent component analysis. *IEEE Transactions on Neural Networks*, *10*(3), 626–634.

Jenkinson, M., Beckmann, C. F., Behrens, T. E., Woolrich, M. W., & Smith, S. M. (2012). FSL. *Neuroimage*, *62*(2), 782–790.

Kalogianni, K., de Munck, J. C., Nolte, G., Vardy, A. N., van der Helm, F. C., & Daffertshofer, A. (2018). Spatial resolution for EEG source reconstruction—A simulation study on SEPs. *Journal of Neuroscience Methods*, *301*, 9–17.

Kantak, S. S., & Winstein, C. J. (2012). Learning–performance distinction and memory processes for motor skills: A focused review and perspective. *Behavioural Brain Research*, *228*(1), 219–231.

Kauranen, K., & Vanharanta, H. (1996). Influences of aging, gender, and handedness on motor performance of upper and lower extremities. *Perceptual and Motor Skills*, *82*(2), 515–525.

Langan, J., Peltier, S. J., Bo, J., Fling, B. W., Welsh, R. C., & Seidler, R. D. (2010). Functional implications of age differences in motor system connectivity. *Frontiers in Systems Neuroscience*, *4*, 17. https://doi.org/10.3389/fnsys.2010.00017

Lange, R. K., Braun, C., & Godde, B. (2006). Coordinate processing during the left-to-right hand transfer investigated by EEG. *Experimental Brain Research*, *168*(4), 547–556. https://doi.org/10.1007/s00221-005-0117-8

Larivière, S., Xifra-Porxas, A., Kassinopoulos, M., Niso, G., Baillet, S., Mitsis, G. D., & Boudrias, M. H. (2019). Functional and effective reorganization of the aging brain during unimanual and bimanual hand movements. *Human Brain Mapping*, *40*(10), 3027–3040.

Levin, O., Fujiyama, H., Boisgontier, M. P., Swinnen, S. P., & Summers, J. J. (2014). Aging and motor inhibition: A converging perspective provided by brain stimulation and imaging approaches. *Neuroscience and Biobehavioral Reviews*, *43*, 100–117. https://doi.org/10.1016/j.neubiorev.2014.04.001

Logothetis, N. K. (2008). What we can do and what we cannot do with fMRI. *Nature*, 453(7197), 869–878.

Maes, C., Gooijers, J., de Xivry, J. J. O., Swinnenab, S. P., & Soisgontier, M. P. (2017). Two hands, one brain, and aging. *Neuroscience and Biobehavioral Reviews*, 75, 234–256. https://doi.org/10.1016/j.neubiorev.2017.01.052

Man'kovskaya, E. P. (2006). Changes in the spectral power and coherence of the EEG alpha rhythm in humans performing grasp efforts by the right and left arm. *Neurophysiology*, 38(3), 197–200. https://doi.org/10.1007/s11062-006-0046-6

Manganotti, P., Gerloff, C., Toro, C., Katsuta, H., Sadato, N., Zhuang, P., ... Hallett, M. (1998). Task-related coherence and task-related spectral power changes during sequential finger movements. *Electroencephalography and Clinical Neurophysiology/Electromyography and Motor Control*, 109(1), 50–62. https://doi.org/10.1016/S0924-980X(97)00074-X

Marcus, D., Harwell, J., Olsen, T., Hodge, M., Glasser, M., Prior, F., ... Van Essen, D. (2011). Informatics and data mining tools and strategies for the human connectome project. *Frontiers in Neuroinformatics*, 5, 4.

Mechsner, F., Kerzel, D., Knoblich, G., & Prinz, W. (2001). Perceptual basis of bimanual coordination. *Nature*, 414(6859), 69–73.

Michel, C. M., & Brunet, D. (2019). EEG source imaging: A practical review of the analysis steps. *Frontiers in Neurology*, 10, 325.

Mima, T., Matsuoka, T., & Hallett, M. (2000). Functional coupling of human right and left cortical motor areas demonstrated with partial coherence analysis. *Neuroscience Letters*, 287(2), 93–96.

Mumford, J. A., Poline, J.-B., & Poldrack, R. A. (2015). Orthogonalization of regressors in fMRI models. *PLoS One*, 10(4), e0126255.

Nasreddine, Z. S., Phillips, N. A., Bédirian, V., Charbonneau, S., Whitehead, V., Collin, I., ... Chertkow, H. (2005). The Montreal Cognitive Assessment, MoCA: A brief screening tool for mild cognitive impairment. *Journal of the American Geriatrics Society*, 53(4), 695–699.

Neuper, C., Wörtz, M., & Pfurtscheller, G. (2006). ERD/ERS patterns reflecting sensorimotor activation and deactivation. *Progress in Brain Research*, 159, 211–222.

Newton, J. M., Sunderland, A., & Gowland, P. A. (2005). fMRI signal decreases in ipsilateral primary motor cortex during unilateral hand movements are related to duration and side of movement. *NeuroImage*, 24(4), 1080–1087. https://doi.org/10.1016/j.neuroimage.2004.10.003

Nichols, T. E., & Holmes, A. P. (2002). Nonparametric permutation tests for functional neuroimaging: A primer with examples. *Human Brain Mapping*, 15(1), 1–25.

Oldfield, R. C. (1971). The assessment and analysis of handedness: The Edinburgh inventory. *Neuropsychologia*, 9(1), 97–113.

Oostenveld, R., Fries, P., Maris, E., & Schoffelen, J.-M. (2011). FieldTrip: Open source software for advanced analysis of MEG, EEG, and invasive electrophysiological data. *Computational Intelligence and Neuroscience*, 2011, 1–9.

Park, D. C., & Reuter-Lorenz, P. (2009). The adaptive brain: Aging and neurocognitive scaffolding. *Annual Review of Psychology*, 60, 173–196.

Pfurtscheller, G. (1981). Central beta rhythm during sensorimotor activities in man. *Electroencephalography and Clinical Neurophysiology*, 51(3), 253–264.

Raichle, M. E. (2001). Cognitive neuroscience: Bold insights. *Nature*, 412(6843), 128–130.

Raichle, M. E. (2015). The brain's default mode network. *Annual Review of Neuroscience*, 38, 433–447.

Repp, B. H. (2005). Sensorimotor synchronization: A review of the tapping literature. *Psychonomic Bulletin & Review*, 12(6), 969–992.

Ritter, P., Becker, R., Graefe, C., & Villringer, A. (2007). Evaluating gradient artifact correction of EEG data acquired simultaneously with fMRI. *Magnetic Resonance Imaging*, 25(6), 923–932.

Ritter, P., Moosmann, M., & Villringer, A. (2009). Rolandic alpha and beta EEG rhythms' strengths are inversely related to fMRI-BOLD signal in primary somatosensory and motor cortex. *Human Brain Mapping*, 30(4), 1168–1187.

Ritter, P., & Villringer, A. (2002). Inhibition and functional magnetic resonance imaging. Paper presented at the International Congress Series, vol. 1235, 213–222.

Ritter, P., & Villringer, A. (2006). Simultaneous Eeg–fmri. *Neuroscience & Biobehavioral Reviews*, 30(6), 823–838.

Robinson, E. C., Garcia, K., Glasser, M. F., Chen, Z., Coalson, T. S., Makropoulos, A., ... Webster, M. (2018). Multimodal surface matching with higher-order smoothness constraints. *NeuroImage*, 167, 453–465.

Robinson, E. C., Jbabdi, S., Glasser, M. F., Andersson, J., Burgess, G. C., Harms, M. P., ... Jenkinson, M. (2014). MSM: A new flexible framework for multimodal surface matching. *NeuroImage*, 100, 414–426.

Rueda-Delgado, L. M., Solesio-Jofre, E., Serrien, D. J., Mantini, D., Daffertshofer, A., & Swinnen, S. P. (2014). Understanding bimanual coordination across small time scales from an electrophysiological perspective. *Neuroscience and Biobehavioral Reviews*, 47, 614–635. https://doi.org/10.1016/j.neubiorev.2014.10.003

Salimi-Khorshidi, G., Douaud, G., Beckmann, C. F., Glasser, M. F., Griffanti, L., & Smith, S. M. (2014). Automatic denoising of functional MRI data: Combining independent component analysis and hierarchical fusion of classifiers. *NeuroImage*, 90, 449–468.

Schirner, M., McIntosh, A. R., Jirsa, V., Deco, G., & Ritter, P. (2018). Inferring multi-scale neural mechanisms with brain network modelling. *eLife*, 7, e28927.

Seidler, R. D., Bernard, J. A., Burutolu, T. B., Fling, B. W., Gordon, M. T., Gwin, J. T., ... Lipps, D. B. (2010). Motor control and aging: Links to age-related brain structural, functional, and biochemical effects. *Neuroscience and Biobehavioral Reviews*, 34(5), 721–733. https://doi.org/10.1016/j.neubiorev.2009.10.005

Serrien, D. J. (2008). Coordination constraints during bimanual versus unimanual performance conditions. *Neuropsychologia*, 46(2), 419–425. https://doi.org/10.1016/j.neuropsychologia.2007.08.011

Serrien, D. J., Cassidy, M. J., & Brown, P. (2003). The importance of the dominant hemisphere in the organization of bimanual movements. *Human Brain Mapping*, 18(4), 296–305. https://doi.org/10.1002/hbm.10086

Sherman, M. A., Lee, S., Law, R., Haegens, S., Thorn, C. A., Hämäläinen, M. S., ... Jones, S. R. (2016). Neural mechanisms of transient neocortical beta rhythms: Converging evidence from humans, computational modeling, monkeys, and mice. *Proceedings of the National Academy of Sciences*, 113(33), E4885–E4894.

Shibata, T., Shimoyama, I., Ito, T., Abla, D., Iwasa, H., Koseki, K., ... Nakajima, Y. (1998). The synchronization between brain areas under motor inhibition process in humans estimated by event-related EEG coherence. *Neuroscience Research*, 31(4), 265–271. https://doi.org/10.1016/S0168-0102(98)00046-7

Shimoyama, I., Ninchoji, T., & Uemura, K. (1990). The finger-tapping test: A quantitative analysis. *Archives of Neurology*, 47(6), 681–684.

Shirazi, S. Y., & Huang, H. J. (2019). More reliable EEG electrode digitizing methods can reduce source estimation uncertainty, but current methods already accurately identify brodmann areas. *Frontiers in Neuroscience*, 13, 1159.

Smith, C. D., Umberger, G., Manning, E., Slevin, J., Wekstein, D., Schmitt, F., ... Kryscio, R. (1999). Critical decline in fine motor hand movements in human aging. *Neurology*, 53(7), 1458–1458, 1461.

Stevenson, C. M., Brookes, M. J., & Morris, P. G. (2011). β-Band correlates of the fMRI BOLD response. *Human Brain Mapping*, 32(2), 182–197.

Stinear, J. W., & Byblow, W. D. (2002). Disinhibition in the human motor cortex is enhanced by synchronous upper limb movements. *The Journal of Physiology*, 543(1), 307–316.

Sullivan, E. V., Adalsteinsson, E., Hedehus, M., Ju, C., Moseley, M., Lim, K. O., & Pfefferbaum, A. (2001). Equivalent disruption of regional white matter microstructure in ageing healthy men and women. *Neuroreport*, 12(1), 99–104.

Sullivan, E. V., & Pfefferbaum, A. (2006). Diffusion tensor imaging and aging. *Neuroscience and Biobehavioral Reviews*, *30*(6), 749–761. https://doi.org/10.1016/j.neubiorev.2006.06.002

Svoboda, J., Sovka, P., & Stancak, A. (2002). Intra- and inter-hemispheric coupling of electroencephalographic 8-13 Hz rhythm in humans and force of static finger extension. *Neuroscience Letters*, *334*(3), 191–195.

Swinnen, S. P. (2002). Intermanual coordination: From behavioural principles to neural-network interactions. *Nature Reviews Neuroscience*, *3*(5), 348–359.

Swinnen, S. P., & Wenderoth, N. (2004). Two hands, one brain: Cognitive neuroscience of bimanual skill. *Trends in Cognitive Sciences*, *8*(1), 18–25.

Toro, C., Cox, C., Friehs, G., Ojakangas, C., Maxwell, R., Gates, J. R., … Ebner, T. J. (1994). 8–12 Hz rhythmic oscillations in human motor cortex during two-dimensional arm movements: Evidence for representation of kinematic parameters. *Electroencephalography and Clinical Neurophysiology/Evoked Potentials Section*, *93*(5), 390–403.

Tscherpel, C., Hensel, L., Lemberg, K., Freytag, J., Michely, J., Volz, L. J., … Grefkes, C. (2020). Age affects the contribution of ipsilateral brain regions to movement kinematics. *Human Brain Mapping*, *41*(3), 640–655.

Van Impe, A., Coxon, J. P., Goble, D. J., Wenderoth, N., & Swinnen, S. P. (2009). Ipsilateral coordination at preferred rate: Effects of age, body side and task complexity. *NeuroImage*, *47*(4), 1854–1862.

van Wijk, B. C., Beek, P. J., & Daffertshofer, A. (2012). Differential modulations of ipsilateral and contralateral beta (de)synchronization during unimanual force production. *The European Journal of Neuroscience*, *36*(1), 2088–2097. https://doi.org/10.1111/j.1460-9568.2012.08122.x

Vecchio, F., Lacidogna, G., Miraglia, F., Bramanti, P., Ferreri, F., & Rossini, P. M. (2014). Prestimulus interhemispheric coupling of brain rhythms predicts cognitive-motor performance in healthy humans. *Journal of Cognitive Neuroscience*, *26*(9), 1883–1890. https://doi.org/10.1162/jocn_a_00615

Vercauteren, K., Pleysier, T., Van Belle, L., Swinnen, S. P., & Wenderoth, N. (2008). Unimanual muscle activation increases interhemispheric inhibition from the active to the resting hemisphere. *Neuroscience Letters*, *445*(3), 209–213. https://doi.org/10.1016/j.neulet.2008.09.013

Wang, B. A., Viswanathan, S., Abdollahi, R. O., Rosjat, N., Popovych, S., Daun, S., … Fink, G. R. (2017). Frequency-specific modulation of connectivity in the ipsilateral sensorimotor cortex by different forms of movement initiation. *NeuroImage*, *159*, 248–260.

Ward, N., & Frackowiak, R. (2003). Age-related changes in the neural correlates of motor performance. *Brain*, *126*(4), 873–888.

SUPPORTING INFORMATION

Additional supporting information may be found in the online version of the article at the publisher's website.

How to cite this article: Chettouf, S., Triebkorn, P., Daffertshofer, A., & Ritter, P. (2022). Unimanual sensorimotor learning—A simultaneous EEG-fMRI aging study. *Human Brain Mapping*, 1–17. https://doi.org/10.1002/hbm.25791